WATPHYS TH-95/01
hep-ph/yymmddd

Adiabatic Analysis of Gravitationally-Induced Three-Flavor Neutrino Oscillations

J. R. Mureika
Department of Physics
University of Waterloo
Waterloo, Ontario N2L 3G1 Canada
[email: newt@avatar.uwaterloo.ca]

R. B. Mann[1]
Department of Applied Mathematics and Theoretical Physics
Silver Street
Cambridge University
Cambridge U.K. CB2 9EW
[email: rbm20@damtp.cam.ac.uk]

Abstract

Some implications of the proposal that flavor nondiagonal couplings of neutrinos to gravity might resolve the solar neutrino problem are considered in the context of three neutrino flavours. Using an adiabatic approximation iso-SNU curves are calculated for the neutrinos which most likely contribute to the observed solar neutrino deficiency. We show that results obtained with two-flavor models can be recovered, and discuss the effects of the addition of a third flavor. Some results are obtained for this case, and these values are compared with recent experimental data.

[1]on leave from Physics. Dept., University of Waterloo, Ontario, Canada

1 Introduction

The Solar Neutrino Problem (SNP) is a mystery which mars our current understanding of stellar astrophysics. There are now four experiments [1, 2, 3, 4] employing different detection techniques that consistently find a deficit in the observed ν_e flux relative to that predicted by various solar models (see *e.g.* those listed in [5]). The origin of this discrepancy is unknown, but various possible solutions based on particle physics techniques have been proposed.

One possible class of solutions to this dilemma invokes oscillations between the various flavors or generations of neutrinos. Perhaps the most elegant solution of this type proposed to date is the Mikheyev-Smirnov-Wolfenstein (MSW) Mechanism [6, 7]; here, the Hamiltonian becomes off-diagonal under a change of eigenbasis for the neutrinos, resulting in flavor-oscillations, much akin to those found in the quark sector. However, the MSW effect requires the neutrinos to possess a mass eigenbasis, and hence implies massive neutrinos.

In 1988, Gasperini [8] conjectured that a similar oscillation phenomenon could take place, while still ensuring massless neutrinos. In this mechanism each neutrino flavor is assumed to couple differently to gravity, permitting flavor oscillations at the expense of violating the equivalence principle. This mechanism has been investigated in a number of papers (see *e.g.* [9, 10, 11]), and has recently been referred to as the VEP mechanism [12]. The results of these studies indicate that, although strongly constrained by existing data, the VEP mechanism is at present a phenomenologically viable means of generating neutrino oscillations.

All investigations of the VEP mechanism to date have restricted consideration to 2-flavor oscillations. However, at our current level of understanding, we know there to be at least three generations of neutrinos. While two-flavor oscillation models are elegant and mathematically simple, it remains a mystery whether or not the τ-neutrino (ν_τ) plays a crucial role in determining the observed ν counting rates and fluxes. Several studies [13, 14, 15, 16, 17] have shown that, for certain cases, a three-flavor analysis can and does contribute interesting physics to the SNP.

In this paper we consider an adiabatic extension of the VEP mechanism to the realistic three-flavor case. The width of the parameter space region found in [12] is reproduced for a two-flavor limit, and the size of the region is

found to shift and/or widen for certain values of the $\nu_e \to \nu_\tau$ mixing angle. Spectra for the solar ^8B neutrinos are produced for differing values of the mixing angles (for fixed violation parameters Δf_{21} and Δf_{31}), both for a fixed ^8B neutrino event rate, as well as for a fixed event rate as would be detected by the ^{37}Cl experiment (*i.e.* combined counting rate for $^8B + ^7Be$ neutrinos). These are compared with the predicted flux in the two-flavor limit.

2 Review of Three-Flavor MSW Neutrino Oscillations

Before proceeding to the gravitational case, we review the MSW mechanism for three flavors. Consider the neutrino eigenbases

$$|\nu_W\rangle = \begin{pmatrix} \nu_e \\ \nu_\mu \\ \nu_\tau \end{pmatrix} \ , \ |\nu_W\rangle = R_3 \, |\nu_M\rangle \ , \tag{1}$$

where $|\nu_W\rangle$ is the weak eigenbasis and $|\nu_M\rangle$ the mass eigenbasis. The matrix R_3 is the 3×3 leptonic analogue of the CKM mixing matrix, which we parametrize as

$$R_3 = e^{i\psi\lambda_7} e^{-i\phi\lambda_5} e^{i\omega\lambda_2} \ , \tag{2}$$

and is proportional the the identity matrix in the case of massless neutrinos. Here ψ, ϕ, ω are three mixing angles, and λ_k the $SU(3)$ generators. For simplicity we have taken R_3 to be real, which implies that there are no CP violations in this sector (*i.e.* the CP-violating phase $\delta = 0$). Including matter effects, and (without loss of generality) assuming $m_3 > m_2 > m_1$, the Hamiltonian in the mass eigenbasis becomes

$$H' = \frac{1}{2} \begin{pmatrix} m_1^2 + m_2^2 + A\, c_\phi^2 - \Delta_N & 0 & A\, s_{2\omega} \sqrt{(1-\beta)/2} \\ 0 & m_1^2 + m_2^2 + A\, c_\phi^2 + \Delta_N & A\, s_{2\omega} \sqrt{(1+\beta)/2} \\ A\, s_{2\omega} \sqrt{(1-\beta)/2} & A\, s_{2\omega} \sqrt{(1+\beta)/2} & 2m_3^2 + 2A\, s_\phi^2 \end{pmatrix} \ . \tag{3}$$

where $c_\phi = \cos\phi$, *etc.* We follow the definitions of [13] with

$$\Delta_N = [(A\, c_\phi^2 - \Delta_\mu\, c_{2\omega})^2 + \Delta_\mu^2 s_{\,2\omega}^{\,2}]^{1/2} \tag{4}$$

$$\beta = \frac{1}{\Delta_N}(A\, c_\phi^2 - \Delta_\mu\, c_{2\omega})^2 \tag{5}$$

where $\Delta_\mu \equiv m_2^2 - m_1^2$, and $A = A(r)$ is the matter interaction term,

$$A(r) = 2\sqrt{2}\, G_F N_e(r) E \ . \tag{6}$$

which describes the interaction of ν_e-neutrinos with solar matter.

From this point on, we make the following substitutions for the mixing angles of (2): $\omega = \theta_{12}$, $\phi = \theta_{13}$, $\psi = \theta_{23}$. Assuming that the the state transitions are adiabatic, we can approximate the ν_e survival probability $P_{\nu_e \to \nu_e}(r, E)$ to be

$$\begin{aligned} P_{\nu_e \to \nu_e}(r, E) &= (1 - P_{LZ2})\, \Theta(A - \Delta_{21}) + P_{LZ2}(1 - P_{LZ3})\, \Theta(\Delta_{21} - A) \\ &\quad \times \Theta(A - \Delta_{31}) + P_{LZ1} P_{LZ3}\, \Theta(\Delta_{31} - A) \ . \end{aligned} \tag{7}$$

Here $\Theta(x)$ is a step function [2], with

$$\Theta(x) = \begin{cases} 1 & \forall x < 0 \\ 0 & \text{otherwise} \end{cases} \ , \tag{8}$$

and P_{LZi} is the Laudau-Zeener "jump" probability for the $\nu_e \to \nu_i$ transition,

$$P_{LZi} = \frac{e^{-\beta_i} - e^{-\alpha_i}}{1 - e^{-\alpha_i}} \ , \tag{9}$$

with

$$\alpha_i = 2\pi\kappa_i \left(\frac{\cos 2\theta_{1i}}{\sin^2 2\theta_{1i}}\right) \ , \ \beta_i = \frac{\pi}{2}\kappa_i(1 - \tan^2\theta_{1i}) \ . \tag{10}$$

For $\nu_e \to \nu_\mu$ transitions, $i = 2$, and $i = 3$ for $\nu_e \to \nu_\tau$.

[2] The step function is a good approximation for the sines and cosines of the matter-enhanced mixing angles, in the case of small vacuum angles [13]. The results obtained using this form of the survival probability are in excellent agreement with the full form of the (adiabatic) probability.

3 Gravitationally-Induced Neutrino Oscillations

We now modify the equations of the previous section to model neutrino oscillations induced by the non-zero difference Δf_{ij} between the gravitational coupling of the different flavors. Consider first the 2-flavor scenario. Let $|\nu_W\rangle$, $|\nu_G\rangle$ be the respective weak and gravitational eigenbases

$$|\nu_W\rangle = \begin{pmatrix} \nu_e \\ \nu_\mu \end{pmatrix} \ , \ |\nu_G\rangle = \begin{pmatrix} \nu_{1G} \\ \nu_{2G} \end{pmatrix}, \tag{11}$$

where the two are related by an $SO(2)$ rotation $R \equiv R(\theta_G)$ (the "mixing" matrix),

$$|\nu_W\rangle = R\,|\nu_G\rangle \ . \tag{12}$$

The gravitational eigenstates obey a variation of the Dirac Equation

$$[i(e_a{}^\mu \gamma^a \partial_\mu) - \zeta(\phi)]|\nu_G\rangle = 0 \ , \tag{13}$$

where $\zeta(\phi)$ is some function of the gravitational potential, which arises due to the non-zero violation of the equivalence principle. For a spherically symmetric metric (choosing angular coordinates $\theta = \phi = 0$ as the trajectory of the neutrino), the vierbeins e^a_μ in (13) reduce the evolution equation to [18]

$$i\frac{d}{dr}|\nu_G\rangle = H\,|\nu_G\rangle \ . \tag{14}$$

where

$$H_i = -2|\phi(r)|E_i(1+f_i) \ . \tag{15}$$

are the diagonal components of the Hamiltonian in the gravitational eigenbasis [11]. Here, $|f_i| \ll 1$ is a (flavor-dependent) parameter which determines the magnitude of the violation of the Einstein Equivalence Principle (EEP). Note that for ν_e (i.e. first generation matter), $f = 0$, which differs from the notation of [12] (in which $f = 1$ represents first-generation neutrinos, which is equivalent to saying that the term $(1 + f) = 1$ in (15)). Under the change of basis $|\nu_G\rangle \to |\nu_W\rangle$, the Hamiltonian becomes off-diagonal,

$$i\frac{d}{dr}|\nu_W\rangle = R^{-1}HR\,|\nu_W\rangle \ , \tag{16}$$

and with the inclusion of weak interactions in the ν_e sector, we obtain the effective Hamiltonian

$$\begin{aligned} H' &= R^{-1}HR + W_e \qquad (17) \\ &= \begin{pmatrix} \frac{\sqrt{2}}{2} G_F N_e(r) - E|\phi(r)|\Delta f \cos 2\theta_G & E|\phi(r)|\Delta f \sin 2\theta_G \\ E|\phi(r)|\Delta f \sin 2\theta_G & 0 \end{pmatrix} \end{aligned}$$

These matter-enhanced oscillations are resonant for complete flavor conversion, which implies the energy condition

$$E = \frac{\sqrt{2}\, G_F N_e(r)}{2|\phi(r)|\Delta f \cos 2\theta_G} \ , \qquad (18)$$

where G_F is the Fermi Coupling Constant, $N_e(r)$ the radial electron number-density, and $\phi(r)$ the dimensionless (solar) gravitational potential. Also, $\Delta f \equiv f_2 - f_1$. In addition, we require the *adiabaticity condition*

$$\kappa = \frac{\sqrt{2}\, G_F \left(N_e\right)_{res} \tan^2 2\theta_G}{\left| \frac{1}{N_e}\frac{dN_e}{dr} - \frac{1}{\phi}\frac{d\phi}{dr} \right|_{res}} \gg 1 \ . \qquad (19)$$

Iso-SNU curves (*i.e.* curves of constant neutrino-counting rates) for 2-flavor gravitationally-induced neutrino oscillations have been carried out in [9], [11], and later repeated in [12]. Two distinct regions of overlap in parameter space were discovered for the given experimental data [12], namely a highly non-adiabatic region (small mixing region), and an adiabatic "large mixing" region. However the authors in [9] have argued that these regions are too small, statistically speaking, to be kept as viable solutions to the SNP for equivalence principle violating neutrino flavors.

4 Extension of VEP Mechanism to Three Flavors

Turning now to the three flavor case, we substitute

$$\frac{1}{2E}\begin{pmatrix} m_1^2 & 0 & 0 \\ 0 & m_2^2 & 0 \\ 0 & 0 & m_3^2 \end{pmatrix} \ \rightarrow \ 2E|\phi(r)|\begin{pmatrix} f_1 & 0 & 0 \\ 0 & f_2 & 0 \\ 0 & 0 & f_3 \end{pmatrix} \ , \qquad (20)$$

which amounts to replacing the mass-squared difference in the probabilities (7) with an EEP violation term,

$$\frac{\Delta m_{ij}^2}{2E} \;\rightarrow\; 2E|\phi(r)|\Delta f_{ij} \;, \tag{21}$$

where $i, j \in [1,3]$, $i \neq j$. For the $\nu_e \rightarrow \nu_e$ survival probability, just the $i = 2, 3$, $j = 1$ terms come into play, and we need only concern ourselves with the mixing angles θ_{12}, θ_{13}.

Of course the entire parameter space $(\Delta f_{21}, \Delta f_{31}, \theta_{12}, \theta_{13})$ is not fair game for this analysis. In particular, we must limit the space to only the areas involving resonances, and which are allowed by adiabatic processes. The physical boundaries on the Δf parameter are easily calculable, and have in the two-flavour case been found to be [12] $\Delta f \in (10^{-18}, 10^{-12})$. The same range holds for the parameters Δf_{ij}. This implies that a ν_e with $|E\Delta f| \geq 10^{-12}$ MeV will not undergo resonance, and will emerge from the sun unscathed, retaining its identity as a ν_e. The other Δf boundary is similar, but for the lower resonance.

This determination of resonant behavior provides us with valuable information. There are now three distinct regions of parameter space which are of physical interest:

1. $\underline{\Delta f_{31} > 10^{-12}, \Delta f_{21} \in (10^{-18}, 10^{-12})}$:
   - Here, we should expect large dependence on $\nu_\mu \rightarrow \nu_e$ transitions (*i.e.* $\Delta f_{21}, \theta_{12}$), as the Δf_{31} parameter puts all transitions to ν_τ above the upper resonance. In the limit $\theta_{13} \rightarrow 0$, we should expect to recover the two-flavor EEP violation model.
2. $\underline{\Delta f_{31} \in ((10^{-18}, 10^{-12}), \Delta f_{21} < 10^{-18}}$:
   - This range represents the opposite of the previous one, where the $\nu_e \rightarrow \nu_\mu$ transitions are not resonant. Hence, we expect to see a two-flavor limit with strong dependence on the $\nu_e \rightarrow \nu_\tau$ transition parameters $(\theta_{13}, \Delta f_{31})$.
3. $\underline{10^{-18} < \Delta f_{21} < \Delta f_{31} < 10^{-12}}$:
   - The most interesting behavior is expected to occur here,where both parameters are sandwiched into the allowed Δf parameter range. Similar to the mass MSW mechanism [17], we

should expect to see dependence on all four parameters in question.

The following section summarizes our analysis of the physically relevant cases #1 and #3.

5 Results

Using the neutrino spectra and solar mass data from [5], as well as the ^{37}Cl and ^{71}Ga cross section data from [19], we have computed iso-SNU rates for case #1 as listed above. The counting rate C_x for a given detector material x with energy threshold E_{min} and absorption cross-section $\sigma_x(E)$ is

$$C_x = \int_0^{R_\odot} dr\, r^2 \xi(r) \int_{E_{min}}^{E_{max}} dE\, \phi(E)\sigma_x(E)P_{\nu_e\to\nu_e}(r,E)\ , \tag{22}$$

for neutrinos with energy spectrum $\phi(E)$ and maximum energy E_{max}. The function $\xi(r)$ represents the fraction of neutrinos of a given type produced at radius r. The rates obtained by numerical intergration of (22) are essentially commensurate with those obtained in ref.[9] and others (*e.g.* see [12]) for the "large mixing region" (to within a few percent). The neutrinos which were assumed to contribute the largest counting rates for each type of detector include, in order of abundance:

- $^{37}Cl \ \rightarrow \ ^{8}B,\ ^{7}Be$
- $^{71}Ga \ \rightarrow \ pp,\ ^{7}Be,\ ^{8}B$.

Note a slight discrepancy in the upper limit of the region as given in [12]. It is believed that any discrepancies could well be the result of numerical errors during calculation, or from minute variations in data for the specific neutrinos. We show in Table 1 the (3σ) adiabatic edges of the parameter space in question, according to the rates as given in [12]:

$$\begin{aligned} C_{Home.} &= 2.55 \pm 0.25\ SNU \\ C_{GALLEX} &= 79 \pm 11.7\ SNU \\ C_{SAGE} &= 73 \pm 19.3\ SNU\ . \end{aligned}$$

The edges of the parameter space region for the Homestake ^{37}Cl detector are roughly equal to the bounds in question, while the 3σ range for the ^{71}Ga experiments is much larger. Hence, the overlap range is determined predominantly by the ^{37}Cl counting rates, which have been calculated to be $\sin^2 2\theta_{12} \in (0.60,\ 0.89)$. This is found to be in close agreement to the range width obtained by [12] of $\sin^2 2\theta_{12} \in (0.60,\ 0.90)$.

As previously mentioned, the most interesting physics is expected to emerge from case #3, where both resonances become crucial in determination of the neutrino behavior. We have obtained some preliminary results for various values of the parameters, using the data for the ^{37}Cl detector. We find that upon inclusion of the third flavor, certain parameters may be chosen such that the "large mixing region" can be widened. To see the magnitude of the widening, we compare the width of the region for 2 flavors to the width using 3 flavors (with two choices of θ_{13}). For the three-flavor model (*i.e.* $\theta_{13} \neq 0$), we choose $\Delta f_{31} = 10^{-15}$.

Table 1: *Width of Allowed Parameter Space for Large Mixing Region as a function of* $\sin^2\theta_{13}$

$\sin^2\theta_{13}$	Width ($\sin^2 2\theta_{12}$)
0	0.60 - 0.89
0.01	0.65 - 0.94
0.05	0.64 - 0.93
0.10	0.63 - 0.93
0.40	0.57 - 0.91

From table 1 we see that the known parameter space overlap for the $\nu_e \rightarrow \nu_\mu$ transitions is shifted and expanded somewhat with the addition of the ν_τ. Further study of the adiabatic behavior of the neutrinos with respect to the SNP may yield a nice set of parameters which maximize the allowed region. Also, we may narrow down our possible choices of violation parameters and mixing angles through a comparison of detected to theoretically calculated ^8B neutrino spectra. *Fig. 1* shows the calculated flux for two of the parameter sets listed in Table 1, for a fixed SNU rate of ^8B neutrinos (i.e. $C = 1.38$

SNU). Note the subtle shifts in shape of each reduced spectrum for the lower half of the energy range, *i.e.* below approximately 6 MeV (*Fig.1*), as well as the flattening of the flux curve for increasing θ_{13} in *Fig.2*. These differences could possibly be differentiated by present-day or near-future detectors (see *e.g.* some discussions in [13, 16, 18]).

A VEP analysis incorporating all three generations of neutrinos seems to yield a greater mobility in parameter space. Such an analysis is quite timely, due to the advent of such new ventures as the Sudbury Neutrino Observatory, for more precise measurements of neutrino fluxes can help determine the right set of parameters. As we can see from *Figs. 1* and *2*, there is greater range of parameters from which to choose such that we can exactly match a flux curve. Since SNO will be able to detect the full solar neutrino flux (flavor-independent via neutral current interactions), studies of such spectra could also help determine the reduction mechanism at work, and hence possibly distinguish between a VEP- or MSW-based phenomenon. Also, an analysis of the non-adiabatic transitions is currently underway, to gauge what effect this will have on the full parameter space range. Since the small mixing region is dominated by highly non-adiabatic transitions, it is believed that this could represent a larger portion of the expanded three-flavor space.

Acknowledgements

J.M. would like to thank Rob Malaney for various insightful discussions. This work was supported by the Natural Sciences and Engineering Research Council of Canada.

References

[1] R. Davis, D. S. Harmer, and K. C. Hoffman, Phys. Rev. Lett. **20**, 1205 (1988).

[2] GALLEX Collaboration, P. Anselmann *et al.*, Phys. Lett. **B327**, 377 (1994).

[3] Kamiokande II Collaboration, K. Hirata *et al.*, Phys. Rev. Lett. **65**, 1297 (1990)

[4] SAGE Collaboration, J. N. Abdurashidov *et al.*, Phys. Lett. **B328**, 234 (1994).

[5] J. N. Bahcall and M. H. Pinsonneault, Rev. Mod. Phys. **64**, 885 (1992).

[6] S. P. Mikheyev and A. Yu. Smirnov, Yad. Fiz. **42**, 1441 (1985).

[7] L. Wolfenstein, Phys. Rev. **D17**, 2369 (1978).

[8] M. Gasperini, Phys. Rev. **D38**, 2635 (1988).

[9] M. N. Butler *et al.*, Phys. Rev. **D47**, 2615 (1993).

[10] A. Halprin and C. N. Leung, Phys. Rev. Lett. **67**, 1833 (1991).

[11] J. Pantaleone, A. Halprin, and C. N. Leung, Phys. Rev. **D47**, R4199 (1993).

[12] J. N. Bahcall, P. I. Krastev, and C. N. Leung, IASSNS-AST 94/54, UDHEP-10-94 (October 1994).

[13] A. Baldini and G. F. Giudice, Phys. Lett. **B186**, 211 (1987).

[14] V. Barger it et al., Phys. Rev. **D22**, 2718 (1980).

[15] M. N. Butler and R. A. Malaney, Phys. Lett. **B283** (1992).

[16] S. P. Mikheyev and A. Yu. Smirnov, Phys. Lett. **B21**, 560 (1988).

[17] H. W. Zaglauer and K. H. Schwarzer, Phys. Lett. **B198** 556 (1987).

[18] H. Minakata and H. Nunokawa, KEK-TH-396/TMUP-HEL-9402, (hep-ph 9405239) (April 1994).

[19] J. N. Bahcall, *Neutrino Astrophysics*, Cambridge University Press, 1988.

Figure Captions

Fig. 1: Plot of reduced ^8B neutrino fluxes ($cm^{-2}s^{-1}MeV^{-1}$) v.s. neutrino energy (MeV) for fixed counting rate $C_{^8B} = 1.38$ SNU showing variation of spectrum shape with choice of parameters. Upper (large) flux is unreduced SSM ^8B flux from [19], while reduced flux curves for 3-flavor model are calculated with $\Delta f_{21} = 10^{-16}$, $\Delta f_{31} = 10^{-15}$, and

- $sin^2 2\theta_{12} = 0.685$; $sin^2\theta_{13} = 0.40$ (dotted)
- $sin^2 2\theta_{12} = 0.70$; $sin^2\theta_{13} = 0.05$ (solid)

These are compared with predicted 2-flavor flux ($\Delta f_{31} \geq 10^{-12}$), with

- $sin^2 2\theta_{12} = 0.697$; $sin^2\theta_{13} = 0$ (dashed)

Fig. 2: Plot of reduced ^8B neutrino fluxes v.s. neutrino energy for fixed counting rate as would be detected by ^{37}Cl experiments (*i.e.* $^8B + {}^7Be$), $C_{Cl} = 2.00$ SNU. Reduced flux curves for 3-flavor model are calculated with $\Delta f_{21} = 10^{-16}$, $\Delta f_{31} = 10^{-15}$, and

- $sin^2 2\theta_{12} = 0.63$; $sin^2\theta_{13} = 0.40$ (dotted)
- $sin^2 2\theta_{12} = 0.693$; $sin^2\theta_{13} = 0.05$ (solid)

These are compared with predicted 2-flavor flux ($\Delta f_{31} \geq 10^{-12}$), with

- $sin^2 2\theta_{12} = 0.701$; $sin^2\theta_{13} = 0$ (dashed)

Fig.1: B8 flux; Fixed Counting Rate

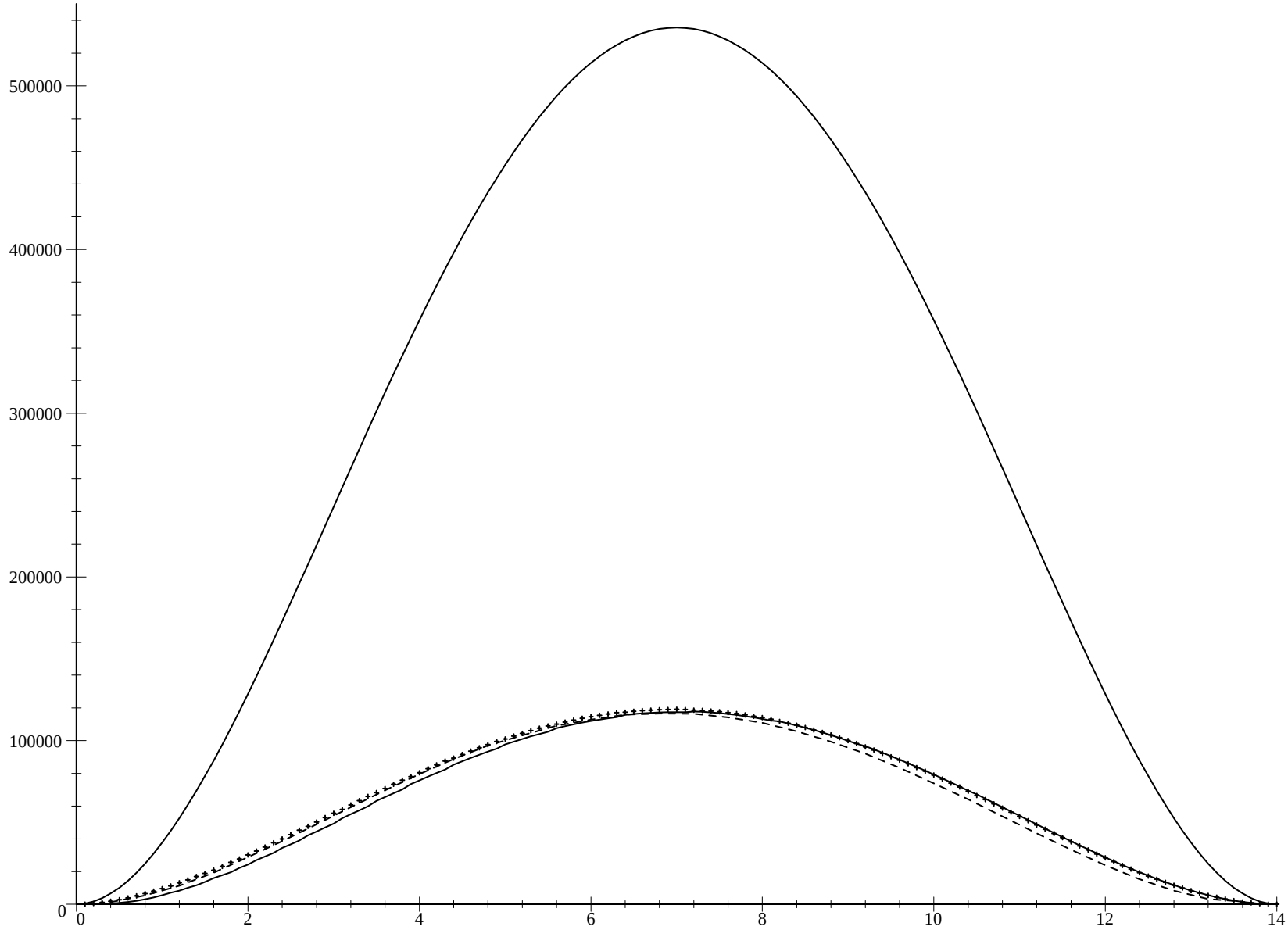

This figure "fig1-1.png" is available in "png" format from:

http://arXiv.org/ps/hep-ph/9501340v1

Fig.2: B8 flux; Fixed Cl Counting Rate

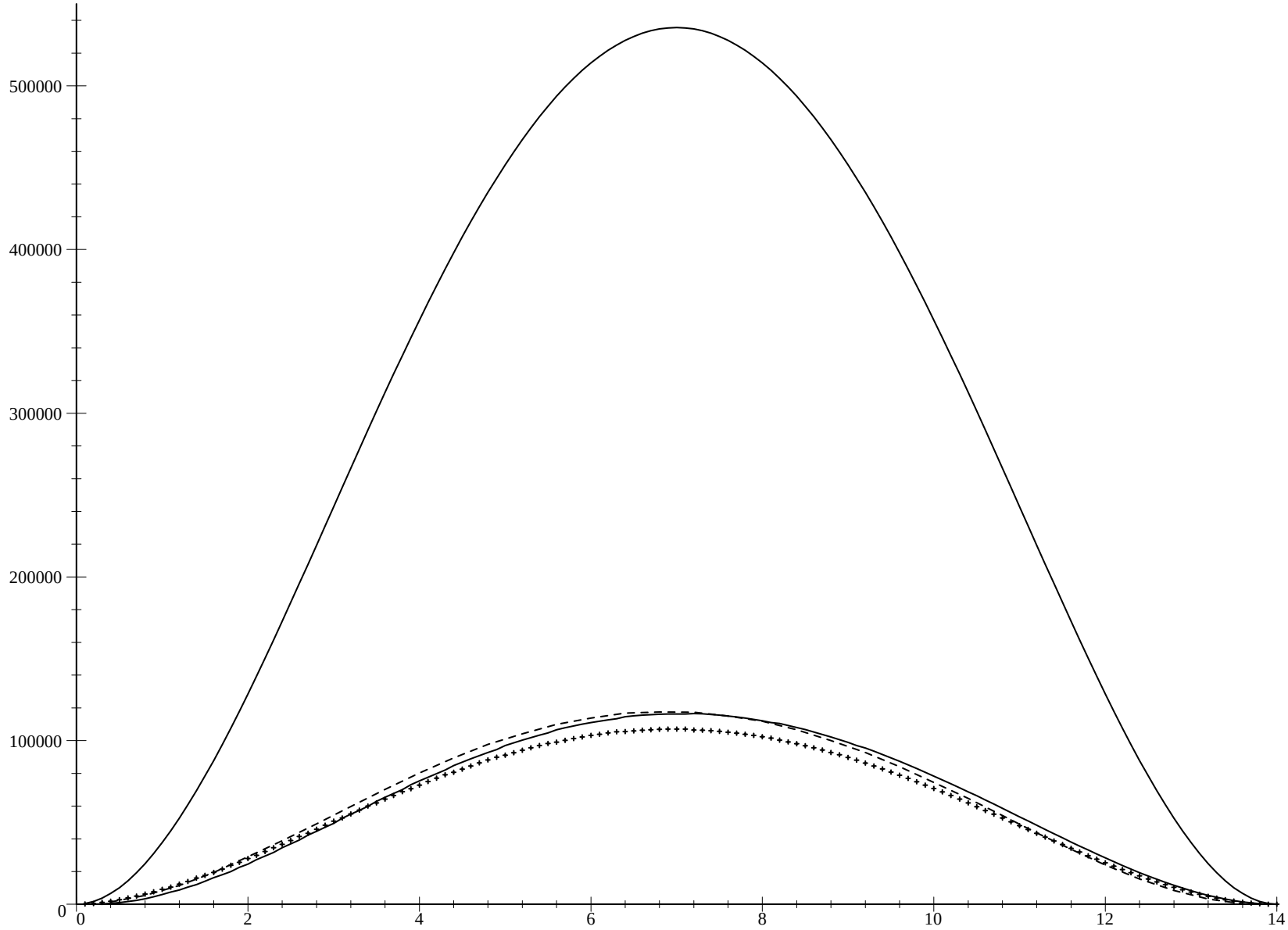

This figure "fig1-2.png" is available in "png" format from:

http://arXiv.org/ps/hep-ph/9501340v1